AIAA SCITECH 2024 Forum, 8-12 January 2024, Orlando, USA. Paper number AIAA 2024-2114
DOI:10.2514/6.2024-2114

Toward Quieter and More Efficient Supersonic Flight: Multi-Objective Optimization of a Bell-Shaped Lift Distribution Wing SSBJ for Low Drag and Low Boom

Giordana Bonavolontà*, Anirudh Manoj †, Cristina Villena Muñoz ‡, Sai Tejesh Chilukuri §, Craig Lawson ¶, Atif Riaz ‖
Cranfield University, Cranfield , United Kingdom, MK430AL

The optimization for low drag and boom of a new promising supersonic aircraft concept is presented in this paper. The Bell-Shaped Lift Distribution wing concept by Prandtl has been explored by the authors to design and optimize a supersonic business jet. This historical concept, known to be a theoretical solution for minimum induced drag wing, has been applied to redesign the SENECA E-19 Supersonic business jet wing. After having demonstrated that a bell span loading operates as intended in the supersonic regime, the configuration so designed has been optimized for low drag and boom by varying fuselage and tail design parameters. In addition, different combinations of engine positions have been also investigated within the optimization loop. The NSGA-II genetic algorithm has been chosen to carry out the multi-objective optimization. Low-to-medium fidelity numerical methods have been implemented to obtain the aerodynamic solution, while in-house multi-level of fidelity tool based on well-known methods has been used to perform sonic boom assessment. Take-off airframe noise assessment has been also performed on the final configuration resulting from optimization. The final configuration shows 6 % increase in aerodynamic efficiency and 7 % in boom with respect to the baseline.

I. Nomenclature

TO	=	Take-Off
$SSBJ$	=	Supersonic Business Jet
$NSGA$	=	Non-dominated Sorting Genetic Algorithm
VLM	=	Vortex Lattice Method
$MTOW$	=	Maximum Take-Off Weight
$MDAO$	=	Multi-disciplinary Analysis and Optimization
$XDSM$	=	eXtended Design Structure Matrix
LE	=	Leading Edge
TE	=	Trailing Edge
SSM	=	Static Stability Margin
Cp	=	Coefficient of pressure
DOE	=	Design of Experiments

II. Introduction

Ever since the retirement of the Concorde in 2003, there have been many efforts and investments to bring back commercial supersonic aviation. This has required extensive scientific research, due to the current increase in environmental concern and regulations still in place that limit supersonic flight. The design of a successful, technically, economically, and environmentally viable supersonic transport aircraft is an extraordinary challenge for the physics

*Doctoral Researcher, School Of Aerospace, Transport and Manufacturing, Cranfield University, g.bonavolonta@cranfield.ac.uk
†MSc Student, School Of Aerospace, Transport and Manufacturing, Cranfield University,anirudhmanoj123@gmail.com
‡Doctoral Researcher, School Of Aerospace, Transport and Manufacturing, Cranfield University, cristina.villena-munoz@cranfield.ac.uk
§MSc Student, School Of Aerospace, Transport and Manufacturing, Cranfield University,saitajesh34@gmail.com
¶Reader in Airframe Systems, School Of Aerospace, Transport and Manufacturing, Cranfield University, c.p.lawson@cranfield.ac.uk
‖Lecturer in Engineering Design, School Of Aerospace, Transport and Manufacturing, Cranfield University, a.riaz@cranfield.ac.uk

of the problem itself leading to conflicting requirements to be managed. As it has been shown in [1], by increasing the Mach number beyond the barrier of 2 meeting all the requirements becomes even harder, and only a technological breakthrough could apparently pave the way for a new era of supersonic commercial aircraft. Many unsuccessful attempts to develop a supersonic airliner have been made over the years, and concepts have been developed, including the Mach 2.7, 250 passengers Boeing 2707 design in the 1960s, the Mach 2.4, 300 passengers HSCT cancelled in 1999, and the Mach 1.7, 4500 nm and 80 passenger Boom Overture. However, many companies, such as Aerion Supersonic, Boom Supersonic, Lockheed Martin, and Northop Grumman (in collaboration with NASA), made great investments in the design of supersonic business jets (SSBJ). It seems, in fact, that this sector of the aviation market could mostly reap the benefits of supersonic flight since time gained is a key factor. Additionally, the smaller size of the SSBJ could make more surmountable certain technical challenges to achieve a feasible proposition. In the end, SSBJ could be used as stepping stones for certain technologies' assessment. The three major issues concerning supersonic aircraft are related to fuel consumption, landing and take-off noise, and sonic boom, and those three have been taken as objectives for the optimization configuration presented in this work. The paper is divided as follows: in Section III, the Prandtl' s bell-shaped lift distribution wing theory is presented, along with its application to a supersonic regime investigated by Manoj [2]. A Business jet aircraft concept implementing a bell-shaped lift distribution wing designed for cruise conditions is also presented. Section IV describes the methodology followed and method and tools implemented to build a multi-disciplinary and optimization framework. In Section V, the results obtained are shown, while VI deals with conclusions and future work.

III. Supersonic Bell Shaped Lift Distribution Wing

In 1933, Prandtl published a work [3] on a new concept of wing that achieves a bell-shaped span loading. He claimed this lift distribution produces the minimum induced drag for a given structural wing weight. This solution (Figure 1) holds the mass of the wing structure constant, and as the load near the wingtip tapers out to zero, the span increases to maintain the weight, increasing the effective aspect ratio of the wing and, hence, reducing the amount of induced drag. Moreover, the bell span load defines a wing with a downwash that changes from heavy downwash at the wing root to upwash towards the wingtip. This particular lift distribution can be achieved by varying both the chord and the geometric twist distribution across the wingspan.

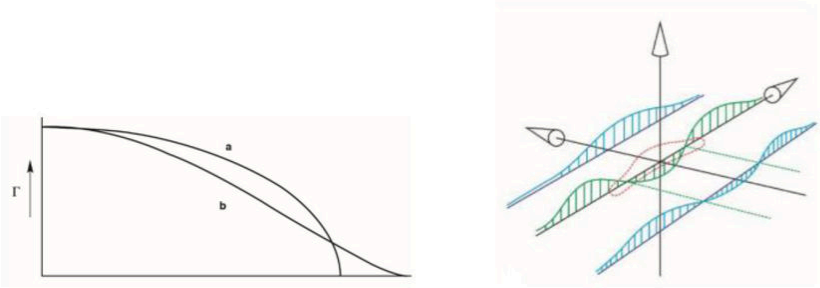

Fig. 1 Bell shaped span loading (left) and bell shaped spanwise downwash distribution (right). Source: [4]).

The bell-shaped wing configuration has been investigated, theoretically tested, and then validated for subsonic aircraft by Al Blowers [5]. He suggests that this unique span load configuration could possibly be extended to supersonic aircraft, provided that the aircraft has a subsonic leading edge to generate the upwash flow field. Manoj explored this possibility in his thesis work [2], performing the conceptual design of a bell-shaped lift distribution wing SSBJ presented in the following subsection.

A. D-1 business jet concept

Figure 2 presents the D-1 business jet used as a baseline for the optimization carried out as the objective of this paper. D-1 is the result of the SENCA E-19 business jet redesign, obtained by the complete redesign of a wing to achieve a bell-shaped lift distribution at cruise. Table 1 summarizes the aircraft's main features.

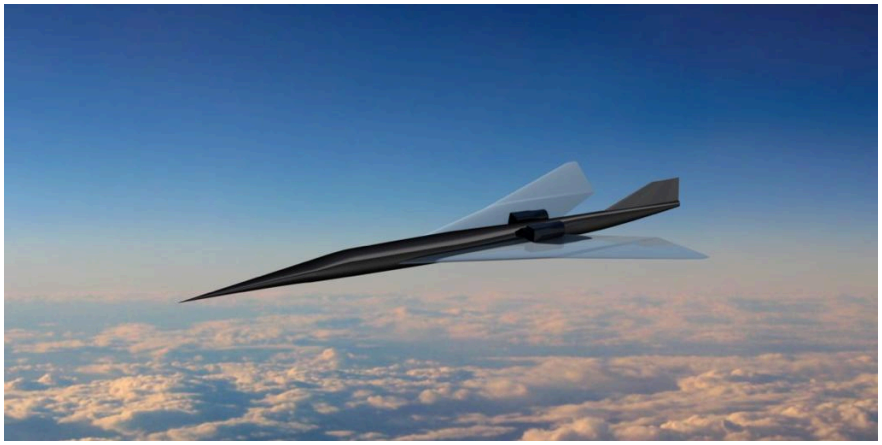

Fig. 2 Baseline aircraft configuration with bell-shaped lift distribution wing.

Table 1 D-1 business jet.

MTOW	45000 kg
Number of passengers	10
Range	4000 nmi
Cruise altitude	50000 ft
Cruise Mach number	1.6
Aerodynamic Efficiency (at cruise)	9
TO Noise Flyover	94.83 dB
TO Noise Sideline	114.67 dB
Sonic Boom Overpressure (at cruise)	0.96 psf
Sonic Boom Perceived Loudness	93 dB

The wing has been designed by assuming fixed values for both sweep angles and surface area, and by iteratively changing both geometrical twist angle and chord distribution until the right amount of lift while producing a bell-shaped lift distribution is achieved.

On a bell-shaped lift distribution wing, well-designed ailerons might create precisely the required amount of pro-verse yaw, eliminating the need for an additional yaw mechanism for a coordinated turning flight. Ailerons could also be used for pitch control, leading to the possibility of entirely remove the horizontal tail. Although the rudder cannot be completely removed since it is required to maintain a certain amount of lateral stability in an engine failure case, the size of the rudder can be reduced to a certain extent, reducing the drag and weight associated with it.

However, these results have been obtained employing low-fidelity methods, and off-design conditions performance has not been tested.

Implementation of bell-shaped lift distribution wing has also shown a reduction in sonic boom overpressure at the ground of about 6% and a gain in aerodynamic efficiency of about 20% in design conditions with respect to the SENECA E-19 baseline level.

In this paper, the wing will be kept as designed to obtain a bell-shaped lift distribution at Mach 1.6, while the fuselage and the tail will be changed to optimize the configuration. Besides, engines' number and their longitudinal position will also be included in the design space, since it is known from the literature review they affect in a significant way the cross-sectional area distribution, and so the wave drag, the sonic boom, and also the noise propagation [6, 7].

IV. Methodology

D-1 business jet concept presented in Section III has been selected as a baseline. The configuration has been optimized for low drag and boom, hence minimization of these values has been the aim of the multi-objective optimization

problem setup.

An MDAO framework has been created in Pyhton. GEMSEO [8], an open-source Generic Engine for Multidisciplinary Scenarios, Exploration and Optimization has been chosen as optimization library. In particular, the plugin created for pymoo library [9] has been exploited to solve the multi-objective optimization problem. Pymoo, in fact, offers state-of-the-art single- and multi-objective optimization algorithms and many more features related to multi-objective optimization such as visualization and decision-making.

Different disciplines have been implemented and linked with each other through coupled variables. A schematic overview of the workflow is provided in Figure 3, while Figure 4 shows the XDSM diagram created in GEMSEO.

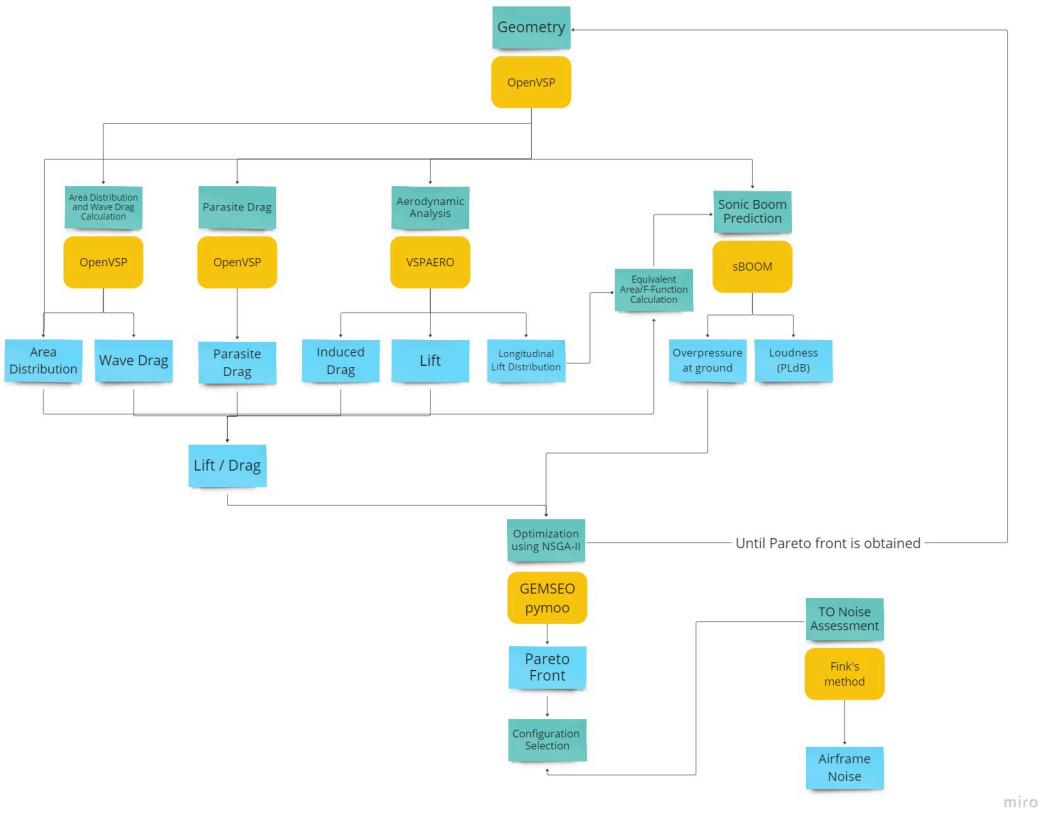

Fig. 3 Schematic view of the methodological approach adopted.

A. Optimization Algorithm: NSGA-II

Multi-objective optimization of the baseline aircraft configuration has been performed by using the NSGA-II Genetic algorithm. A genetic algorithm is a method to solve optimization problems based on natural selection. The genetic algorithm repeatedly modifies a population of individual solutions. At each step, individuals from the current population are selected to be parents and are used to produce children for the next generation. Over successive generations, the population "evolves" toward an optimal solution. NSGA follows the general outline of a genetic algorithm with a modified mating and survival selection. In NSGA-II, first, individuals are selected frontwise. By doing so, there will be a situation where a front needs to be split because not all individuals are allowed to survive. In this splitting front, solutions are selected based on crowding distance.

NSGA-II algorithm has been widely used for aircraft design optimization [10–12] where the optimal solution is often the result of weighing multiple factors and conflicting requirements. No single solution in fact exists for multi-objective optimization problems, but a set of non-dominated optimal results should be found, as well the so-called Pareto optimal front (Figure 5).

B. Disciplines

Three disciplines have been implemented within the framework: geometry, aerodynamics and sonic boom. A brief explanation of the methods and tools implemented for each discipline is provided in the following subsections.

1. Geometry

The aircraft geometry is generated in OpenVSP [14]. Starting from the baseline configuration, geometrical dimensions and parameters for each component are modified according to the optimization iteration. The wing remains fixed since its shape has been previously designed to achieve a bell-shaped lift distribution in cruise conditions.

2. Aerodynamics

Aerodynamic analysis has been performed by using the VSPAERO VLM method [15] included in OpenVSP. It has been wrapped in the Python framework by means of a dedicated Python module. This solution has retained a good compromise between the accuracy of results and the computational cost. In particular, since the optimization problem has been performed only for supersonic cruise conditions, the supersonic linearised theory at the base of the VLM applies. Lift coefficient, induced drag coefficient and longitudinal lift distribution are the outputs provided by this discipline. In particular, in order to obtain the lift distribution along the x-axis, modifications of the VSPAERO slicer source code have been made by the authors. In fact, by providing the cut sections definition file with the Mach angle, planes rotated with respect to the longitudinal axis by this angle can be generated, and the pressure coefficient calculated. The lift coefficient for each X section is then easily obtained by integrating the pressure coefficient (Cp) over the section's length (Equation 1 in which ρ is the density, V is the speed, S is the wing area).

$$l(x) = -\frac{1}{2}\rho V^2 c \int_{-y(x)}^{y(x)} \Delta Cp(y,z)dx \tag{1}$$

Parasite drag coefficient is obtained by a specific OpenVSP module that implements the form factor method [16], while wave drag coefficient is calculated by another OpenVSP module implementing supersonic area rule [17]. Cross-sectional area is also generated by the wave drag module. In Figure 6, an example of cross-sectional area distribution obtained by cutting the aircraft with Mach planes (planes inclined by Mach angle with respect to the longitudinal axis) is provided.

3. Sonic Boom

Sonic Boom prediction is performed in two steps: near-field pressure distribution calculation and signal propagation to the ground (Figure 7). In this work, the sonic boom prediction has been carried out by a multi-fidelity, in-house developed software that implements Carlson's method (low fidelity), VLM (medium fidelity), and CFD-based (high fidelity) surrogate models for near-field signature generation, and NASA licensed software sBOOM [18] for signature propagation through the atmosphere. A complete review of sonic boom prediction methods is given in [19]. The output from this discipline is the maximum overpressure at the ground. Figure 8 shows the near-field signature and ground signature produced by the D-1 baseline aircraft configuration in cruise at 50000 ft.

sBOOM is also able to calculate different boom loudness metrics by post-processing the signal content. In particular, A-weighted Sound Exposure Level (SELa), B-weighted Sound Exposure Level (SELb), C-weighted Sound Exposure Level (SELc), D-weighted Sound Exposure Level (SELd), and Perceived Loudness (PL). Both overpressure and loudness could be used as optimization objectives [20], but since overpressure is directly linked to the aircraft shape, it is commonly chosen for configuration optimization.

4. Take-Off Noise

Take-off airframe noise has been calculated for both the baseline and the final optimal configuration by means of an in-house developed tool that implements Fink's method [22].

C. Design Variables

Design variables have been selected within the most important geometrical aircraft parameters known to affect drag and boom levels the most. Table 2 lists the set of design variables along with baseline values and boundaries used for this optimization problem. Figure 9 clarifies the definition of fuselage's design variables. Engines number and positions

have been treated as a unique dummy variable (x8 in the state vector) that identifies an engine configuration, ranging from 1 to 4, and showed in Figure 10.

Table 2 Design variables selected for the optimization problem.

DESIGN PARAMETERS				
Parameter	**Variable**	**Baseline Value**	**Lower Value**	**Upper Value**
Fuselage				
Length	x1	45 m	30 m	60 m
Max Diameter	x2	2 m	1 m	3 m
Nose Angle	x3	3 deg	0 deg	5 deg
Tail Angle	x4	3 deg	0 deg	5 deg
Wing				
Longitudinal position/ fuselage length	x5	45%	20%	60%
Vertical Tail				
Sweep Angle	x6	66 deg	50 deg	70 deg
Area/Wing Area	x7	12%	10%	25%

D. Constraints

Some constraints have been included in the definition of the optimization problem. There are several categories of constraints that can be defined: geometrical constraints, aerodynamic constraints, performance constraints, and others. Moreover, constraints could be linear or nonlinear, and of equal (=) or in-equal (<,>) type. In this particular problem, linear inequality constraints are defined. They are reported in Table 3: c1, c2, c3 are geometrical constraints, aimed at obtaining a feasible aircraft configuration, while a constraint on the longitudinal Static Stability Margin has been added to avoid the aircraft becoming unstable due to wing repositioning.

Table 3 Constraints for the optimization problem.

CONSTRAINTS	
c1	wing_{TE} < Fuselage length
c2	Fuselage Max Diameter > Min Diameter*
c3	Cabin Length > Min Cabin Length*
c4	SSM > 0.05

***: Minimum Diameter and Cabin length are calculated to accomodate 10 passengers. Details in [2]**

V. Results

A. Sensitivity Analysis

To define an optimization scenario that is well suited for the problem, sensitivity analysis is required. Sensitivity analysis allows the identification of the parameter or set of parameters that have the greatest influence on the model output/s. It consequently provides useful insight into which model input contributes most to the variability of the model output(s) [23]. The result of the analysis provides indications about the variables that have to be retained for the following optimization process and several information that can be exploited in the analysis of the optimal final solutions. Sensitivity analysis could be qualitative or quantitative, local or global. In this work, a global sensitivity analysis has been conducted. In a global sensitivity analysis, all parameters are varied simultaneously over the entire parameter space, which allows to simultaneously evaluate the relative contributions of each individual parameter as well

as the interactions between parameters to the model output variance. Sobol's method has been chosen and Sobol's indices have been calculated.

1. Scatter Plot Matrix

A Scatter Plot Matrix has been generated by performing a DOE in GEMSEO. Latin Hypercube [24] has been chosen as the sampling algorithm and 30 samples have been generated.

In Figure 11, a clear trend can be seen between the output and fuselage diameter (x4) and nacelle configuration (x8). It is easy to guess that the variance of the drag coefficient is strongly influenced by these two variables.

In Figure 12, instead, there is a recognizable trend among the overpressure values and the fuselage length (x1) and diameter (x4), wing position (x5) and nacelle configuration (x8). Since sonic boom is due to volume and lift distribution, every design variable that affects these two variables has an impact on the overpressure value reached at the ground.

2. Sobol sensitivity analysis

Sobol's method [25, 26] is a method based on the decomposition of the model output variance into the sum of variances of the input parameters in increasing dimensionality [23, 27]. Sobol's sensitivity analysis determines the contribution of each input parameter and its interactions with the overall model output variance. In other words, the analysis is intended to determine how much of the variability in model output is dependent upon each of the input parameters, either upon a single parameter or upon an interaction between different parameters. The decomposition of the output variance in Sobol's method employs the same principle as the classical analysis of variance in a factorial design. Results from the analysis are sensitivity indices, and in particular first order, second order and total indices are calculated. They are then used to rank the design variable and to perform a screening. First-order sensitivity indices are used to measure the fractional contribution of a single parameter to the output variance. Second-order sensitivity indices are used to measure the fractional contribution of parameter interactions to the output variance. Total-order sensitivity indices take into account both the main, second-order, and higher-order effects, which involve the evaluation over a full range of parameter space. The higher the sensitivity indices value, the more influential the respective model parameters and the associated steps are. Although no distinct cutoff value has been defined, the rather arbitrary value of 0.05 is frequently accepted for this type of analysis for distinguishing important from unimportant parameters [28].

Sobol sensitivity analysis has been performed for both objective functions (CD (drag coefficient) and Overpressure) by using SAlib open source python library [29, 30]. Saltelli's sampling method [31, 32] has been used to generate 144 samples. Results are shown in Figures 13 14.

Figure 13 shows total, first and second indices for the drag coefficient. As can be seen in the first indices plot (S1), all the variables have an impact on the output except the fuselage length (x1) and the nose angle (x2). They present, in fact, negative indices. This is due to numerical errors: a better result could be obtained by increasing the number of samples. However, since their total indices (ST) are positive and higher than the usual threshold value of 0.05, all the variables are retained to explain the variance of the drag coefficient overall. The second indices plot shows also there is a quite strong interaction between all the parameters studied. Modifications of the cabin section diameter (x4) act on the aft-body interference drag due to the central fuselage. In particular, an increase in the section radius increases the drag coefficient. The increase of the nose slope (x1) introduces an increase in the effective angle of attack seen by the nose of the fuselage, increasing in this way the fuselage drag, but at the same time increasing the lift produced. Modifications of the wing position (x5) directly act on the cross-sectional area rule, having a strong impact on the volume wave drag. However, higher modifications in drag coefficients could be obtained by varying wing parameter that in this case has not been modified.

When it comes to overpressure values, according to Figure 14 all the variables can be considered important overall, although fuselage length (x1), tail angle (x3), fuselage diameter (x4) and wing position (x5) first-order indices resulted to be lower than the threshold values. Regarding interaction, nose angle (x2) variation with both tail angle (x3) and fuselage diameter (x4) generate the highest values. The cabin diameter (x4) plays a primary role in defining the magnitude of the acoustic cost function. Modifications of the cabin geometry have an impact on the middle-aft part of the acoustic signal. In particular, a decreased cabin diameter produces a more extended expansion zone before the wing shock, while an increase limits the flow acceleration after the front shock and an additional shock occurs just before the wing leading edge shock [20]. Wing position (x5) also has a strong impact on the ground signature: As the wing is displaced towards the front part of the aircraft, the related pressure peak in the near-field signature approaches the nose pressure peak. During the propagation, the two shocks tend to coalesce resulting in a N-wave signature. The front shock overpressure is increased compared to the reference configuration. A rear wing, due to the interference with the rear fuselage, results

in a configuration with increased lift. The acoustic performance is not improved due to the creation of an additional rear shock. The other parameter that has a strong effect on the acoustic performance is the nose deflection angle (x2). A nose deflection downward deviates the flow-field in the region above the aircraft thus reducing the nose shock wave directed towards the ground with a beneficial effect on the ground signature front overpressure. Furthermore, the expansion wave just before the wing is reduced. As a consequence, the configuration with a nose deflected downward also shows a reduction of the wing shock magnitude thus providing a considerable improvement in the acoustic performance. The opposite occurs for an upward nose deflection.

B. Optimization

C. Configuration Selection and Comparison with the baseline

After having obtained the Pareto front, which includes all the non-dominated solutions, a unique configuration should be selected. There are several methods to make this selection [33–36] but since both objectives are equally important, the easiest and most straightforward one is to measure the distance from each of the Pareto front solutions to the utopian point (orange point in Figure 15) and choose the one with minimum distance. Assuming to take the CD and overpressure values from each individual solution and combining with CD and overpressure taking the values from the other solutions, the best solution that can be obtained under the assumption is called the utopian point. As the name suggests, it is unrealistic. But it provides a good reference for how far away each Pareto front solution is from this ideal solution.

Figure 16 shows a graphic comparison between the baseline and the optimal aircraft configuration, while in Table 4, the final values for the design variables are reported to be compared with the baseline ones. The configuration resulting from the optimization problem resolution shows a slightly longer and bigger fuselage, bigger vertical tail, higher nose angle and lower tail angle. Moreover, the four over-the-wing engine configuration substitutes the twin-engine configuration.

Table 4 Design variables values for the baseline and the optimal configuration.

Design Variable	D-1	Optimal solution
Fuselage length	45 m	46 m
Max diameter	2 m	2.1 m
Nose Angle	3 deg	2 deg
Tail Angle	3 deg	3.4 deg
Wing longitudinal position/fuselage length	45%	43%
Vertical Tail Sweep Angle	66 deg	63 deg
Vertical Tail Area/Wing Area	12%	14%
Nacelle Configuration	Twin-Engine	Quad-Engine

Table 5 compares the initial and final configuration performance. The optimized configuration shows an increase in aerodynamic efficiency of 6% and a reduction in both maximum ground overpressure and perceived loudness of respectively 7% and 3%. The airframe take-off noise does not change from the baseline to the optimized configuration, since it is mainly driven by the wing that has been taken as it is.

Table 5 D-1 business jet compared with optimal solution.

	D-1	Optimal solution
MTOW	45000 kg	45000 kg
Number of passengers	10	10
Range	4000 nmi	4000 nmi
Cruise altitude	50000 ft	50000 ft
Cruise Mach number	1.6	1.6
Aerodynamic Efficiency (at cruise)	9	9.6
TO Noise Flyover	94.83 dB	94.83 dB
TO Noise Sideline	114.67 dB	114.67 dB
Sonic Boom Overpressure (at cruise)	0.96 psf	0.89 psf
Sonic Boom Perceived Loudness	93 dB	90 dB

VI. Conclusions

A multi-objective shape optimization has been performed on a bell-shaped lift distribution SSBJ innovative configuration. The wing, designed to obtain such lift distribution in on-design conditions has been kept fixed, while the fuselage and tail shape have been changed to find out the Pareto front solution for low drag and low sonic boom overpressure at ground. Engines' configuration has also been included as a design variable into the optimization loop since it affects both outcomes. The optimized configuration presents a longer and slightly bigger fuselage, lower nose angle, higher tail angle, and bigger vertical tail. The wing is positioned a bit ahead and a quad over-the-wing engine configuration is selected to replace the twin-engine configuration of the baseline. The results obtained by using multi-level of fidelity tools show an increase in cruise aerodynamic efficiency of 6% (hence a reduction of the total drag coefficient) and a reduction in both boom overpressure and loudness at ground of 7% and 3% respectively. In future works, a complete optimization loop will be performed by also changing wing parameters and including LTO noise assessment as a third objective.

Acknowledgments

This project has received funding from the European Union‘s Horizon 2020 research and innovation program under grant No 101006742.

References

[1] Council, N. R., et al., *Commercial Supersonic Technology: The Way Ahead*, National Academies Press, 2002.

[2] Manoj, A., "CONCEPTUAL DESIGN OF A NOVEL LOW BOOM LOW DRAG SUPERSONIC BUSINESS JET- ON WINGS OF MINIMUM INDUCED DRAG," , 2021.

[3] Prandtl, L., "About Smallest Induced Drag of A [n Air Plane] Wing," *Zeitschrift Fur Flugtechnik Und Motorluftschiffahrt*, 1933, pp. 305–06.

[4] Bowers, A. H., Murillo, O. J., Jensen, R. R., Eslinger, B., and Gelzer, C., "On wings of the minimum induced drag: Spanload implications for aircraft and birds," Tech. rep., 2016.

[5] Bowers, A. H., Murillo, O. J., Berger, D. E., Hawkins, V. S., Newton, L. J., Waddell, A. G., Glover, E. D., Brady, J. C., Bodylski, J. K., Bowers, R. A., et al., "Experimental Flight Validation of the Prandtl 1933 Bell Spanload," 2021.

[6] Howe, D., "Engine placement for sonic boom mitigation," *40th AIAA Aerospace Sciences Meeting & Exhibit*, 2002, p. 148.

[7] UENO, A., and WATANABE, Y., "Propulsion/airframe Integration Considering Low Drag and Low Sonic Boom," *29th Congress of the International Council of the Aeronautical Sciences*, 2014.

[8] Gallard, F., Vanaret, C., Guénot, D., Gachelin, V., Lafage, R., Pauwels, B., Barjhoux, P.-J., and Gazaix, A., "GEMS: A Python Library for Automation of Multidisciplinary Design Optimization Process Generation," *2018 AIAA/ASCE/AHS/ASC Structures, Structural Dynamics, and Materials Conference*, 2018.

[9] Blank, J., and Deb, K., "pymoo: Multi-Objective Optimization in Python," *IEEE Access*, Vol. 8, 2020, pp. 89497–89509.

[10] Wang, Y., Yin, H., Zhang, S., and Yu, X., "Multi-objective optimization of aircraft design for emission and cost reductions," *Chinese Journal of Aeronautics*, Vol. 27, No. 1, 2014, pp. 52–58.

[11] Andersson, J., and Krus, P., "A multi-objective optimization approach to aircraft preliminary design," *SAE transactions*, 2003, pp. 454–460.

[12] Xu, L., Zhang, B., Chen, B., and Wu, P., "Multi-Objective Optimization Design of Liftbody Aircraft Using Kriging Model," *Journal of Physics: Conference Series*, Vol. 1985, IOP Publishing, 2021, p. 012034.

[13] Deb, K., and Sinha, A., "An efficient and accurate solution methodology for bilevel multi-objective programming problems using a hybrid evolutionary-local-search algorithm," *Evolutionary computation*, Vol. 18, No. 3, 2010, pp. 403–449.

[14] McDonald, R. A., "Advanced modeling in OpenVSP," *16th AIAA Aviation Technology, Integration, and Operations Conference*, 2016, p. 3282.

[15] OpenVSP Ground School, "VSPAERO Basics," `https://vspu.larc.nasa.gov/training-content/chapter-3-model-analysis-in-openvsp/vspaero-basics/`, 2022. Accessed: 2023-11-01.

[16] Gur, O., Mason, W. H., and Schetz, J. A., "Full-configuration drag estimation," *Journal of Aircraft*, Vol. 47, No. 4, 2010, pp. 1356–1367.

[17] Harris Jr, R. V., "An analysis and correlation of aircraft wave drag," *National Aeronautics and Space Administration*, 1964.

[18] Rallabhandi, S. K., "Advanced sonic boom prediction using the augmented Burgers equation," *Journal of Aircraft*, Vol. 48, No. 4, 2011, pp. 1245–1253.

[19] Bonavolontà, G., Lawson, C., and Riaz, A., "Review of Sonic Boom Prediction and Reduction Methods for Next Generation of Supersonic Aircraft," *Aerospace*, Vol. 10, No. 11, 2023, p. 917.

[20] Minelli, A., "Aero-acoustic shape optimization of a supersonic business jet," Ph.D. thesis, Université Nice Sophia Antipolis, 2013.

[21] Abraham, T. A., "Sonic Boom Loudness Reduction Through Localized Supersonic Aircraft Equivalent-Area Changes," Ph.D. thesis, Utah State University, 2021.

[22] Fink, M. R., "Airframe noise prediction method," Tech. rep., United Technologies Research Center East Hartford CT, 1977.

[23] Saltelli, A., Chan, K., and Scott, E., "Sensitivity analysis., Wiley Series in Probability and Statistics.(Wiley: New York)," 2000.

[24] Wikipedia, "Latin Hypercube Sampling," https://en.wikipedia.org/wiki/Latin$_hypercube_sampling$, 2023. $Accessed$: 2023 – 11 – 06.

[25] Sobol, I. M., "Global sensitivity indices for nonlinear mathematical models and their Monte Carlo estimates," *Mathematics and computers in simulation*, Vol. 55, No. 1-3, 2001, pp. 271–280.

[26] Soboĺ, I., "Sensitivity estimates for nonlinear mathematical models," *Math. Model. Comput. Exp.*, Vol. 1, 1993, p. 407.

[27] Saltelli, A., Tarantola, S., and Chan, K.-S., "A quantitative model-independent method for global sensitivity analysis of model output," *Technometrics*, Vol. 41, No. 1, 1999, pp. 39–56.

[28] Zhang, X.-Y., Trame, M. N., Lesko, L. J., and Schmidt, S., "Sobol sensitivity analysis: a tool to guide the development and evaluation of systems pharmacology models," *CPT: pharmacometrics & systems pharmacology*, Vol. 4, No. 2, 2015, pp. 69–79.

[29] Iwanaga, T., Usher, W., and Herman, J., "Toward SALib 2.0: Advancing the accessibility and interpretability of global sensitivity analyses," *Socio-Environmental Systems Modelling*, Vol. 4, 2022, p. 18155. https://doi.org/10.18174/sesmo.18155, URL https://sesmo.org/article/view/18155.

[30] Herman, J., and Usher, W., "SALib: An open-source Python library for Sensitivity Analysis," *The Journal of Open Source Software*, Vol. 2, No. 9, 2017. https://doi.org/10.21105/joss.00097, URL https://doi.org/10.21105/joss.00097.

[31] Saltelli, A., "Making best use of model evaluations to compute sensitivity indices," *Computer physics communications*, Vol. 145, No. 2, 2002, pp. 280–297.

[32] Campolongo, F., Saltelli, A., and Cariboni, J., "From screening to quantitative sensitivity analysis. A unified approach," *Computer physics communications*, Vol. 182, No. 4, 2011, pp. 978–988.

[33] Wang, Z., and Rangaiah, G. P., "Application and analysis of methods for selecting an optimal solution from the Pareto-optimal front obtained by multiobjective optimization," *Industrial & Engineering Chemistry Research*, Vol. 56, No. 2, 2017, pp. 560–574.

[34] Rao, R., and Lakshmi, R., "Ranking of Pareto-optimal solutions and selecting the best solution in multi-and many-objective optimization problems using R-method," *Soft Computing Letters*, Vol. 3, 2021, p. 100015.

[35] Li, M., Chen, T., and Yao, X., "How to evaluate solutions in Pareto-based search-based software engineering: A critical review and methodological guidance," *IEEE Transactions on Software Engineering*, Vol. 48, No. 5, 2020, pp. 1771–1799.

[36] Chaudhari, P., Dharaskar, R., and Thakare, V., "Computing the most significant solution from Pareto front obtained in multi-objective evolutionary," *International Journal of Advanced Computer Science and Applications*, Vol. 1, No. 4, 2010.

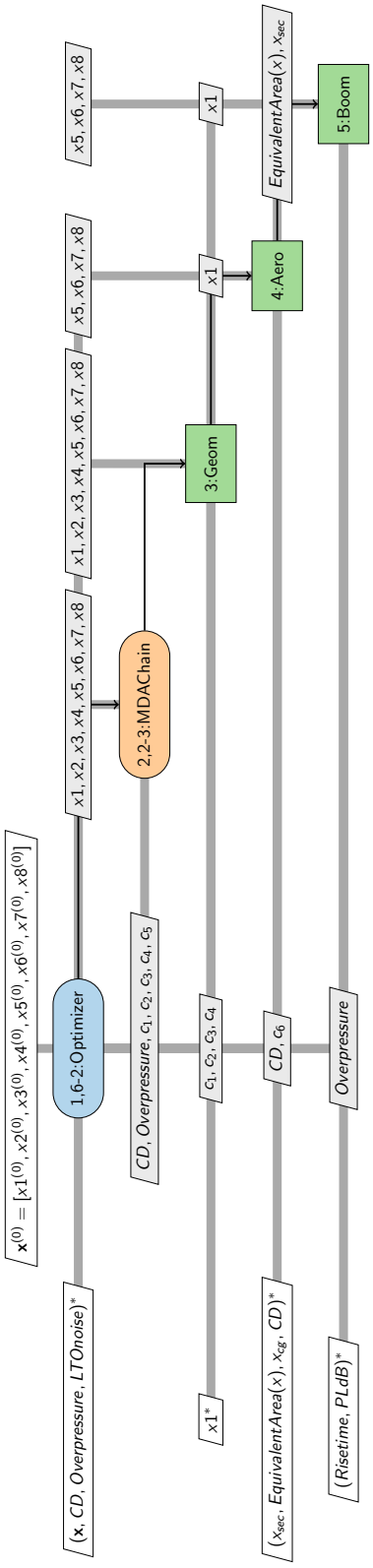

Fig. 4 XDSM created in GEMSEO to visualize the MDO process built.

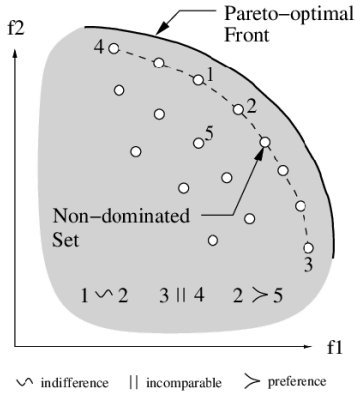

Fig. 5 Non dominated set of optimal solutions and Pareto front [13].

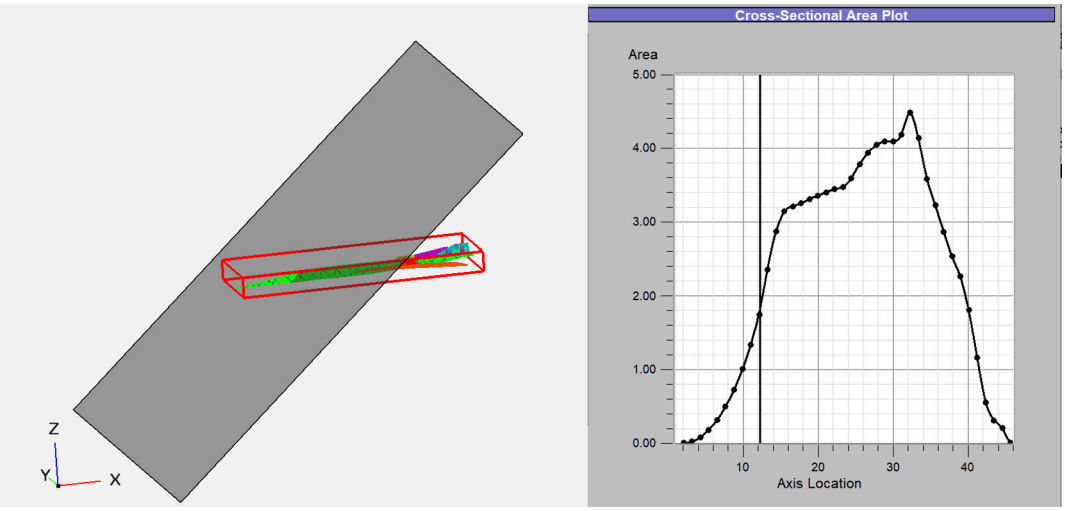

Fig. 6 D-1 business jet cut by Mach planes (left), cross-sectional area distribution (right).

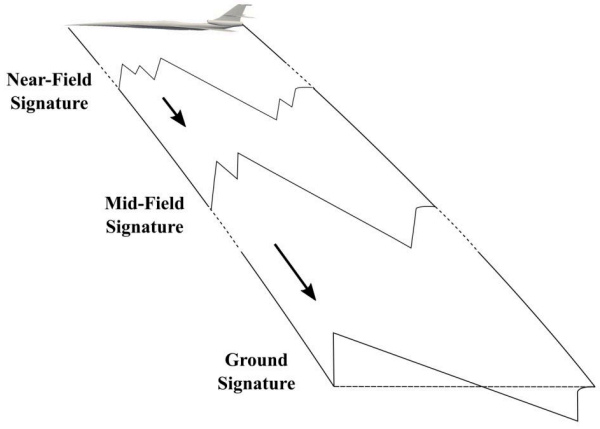

Fig. 7 Sonic boom generation and propagation to the ground (Source: [21]).

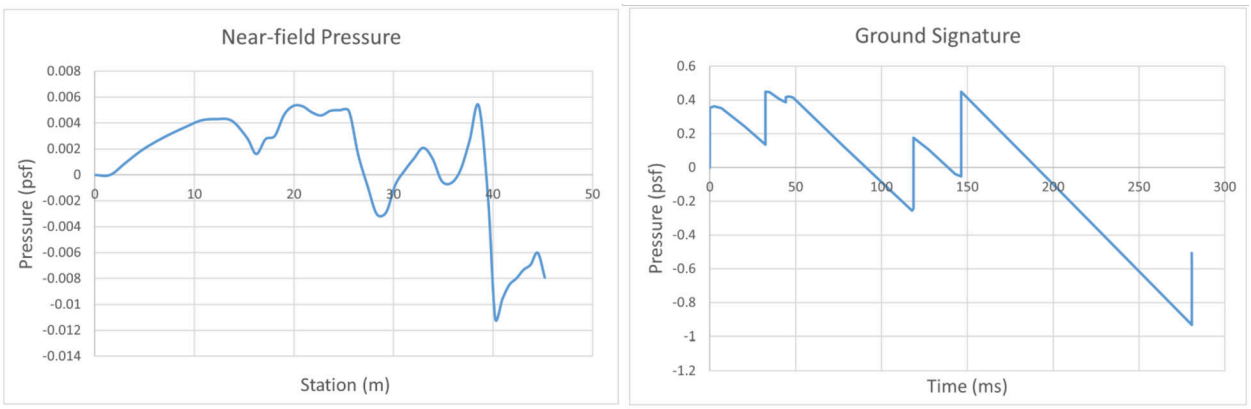

Fig. 8 D-1 Near-field pressure distribution generated around the aircraft in cruise (55000 ft) (up), and pressure signature at the ground (down).

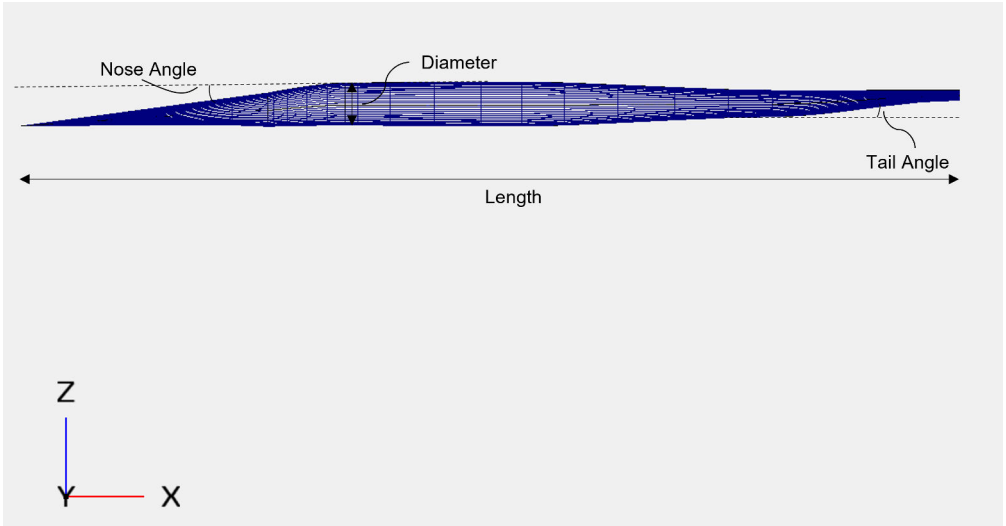

Fig. 9 Fuselage design parameters definition.

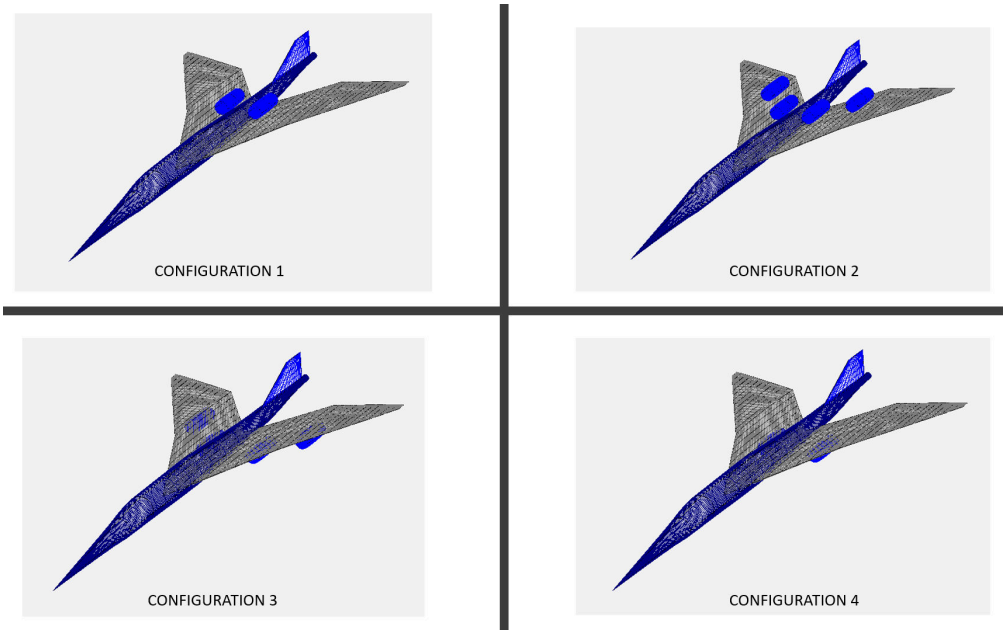

Fig. 10 Engine configurations analysed: on the wing twin engine (CONF1), on the wing quad engine (CONF2), under the wing quad engine (CONF3), under the wing twin engine (CONF4) .

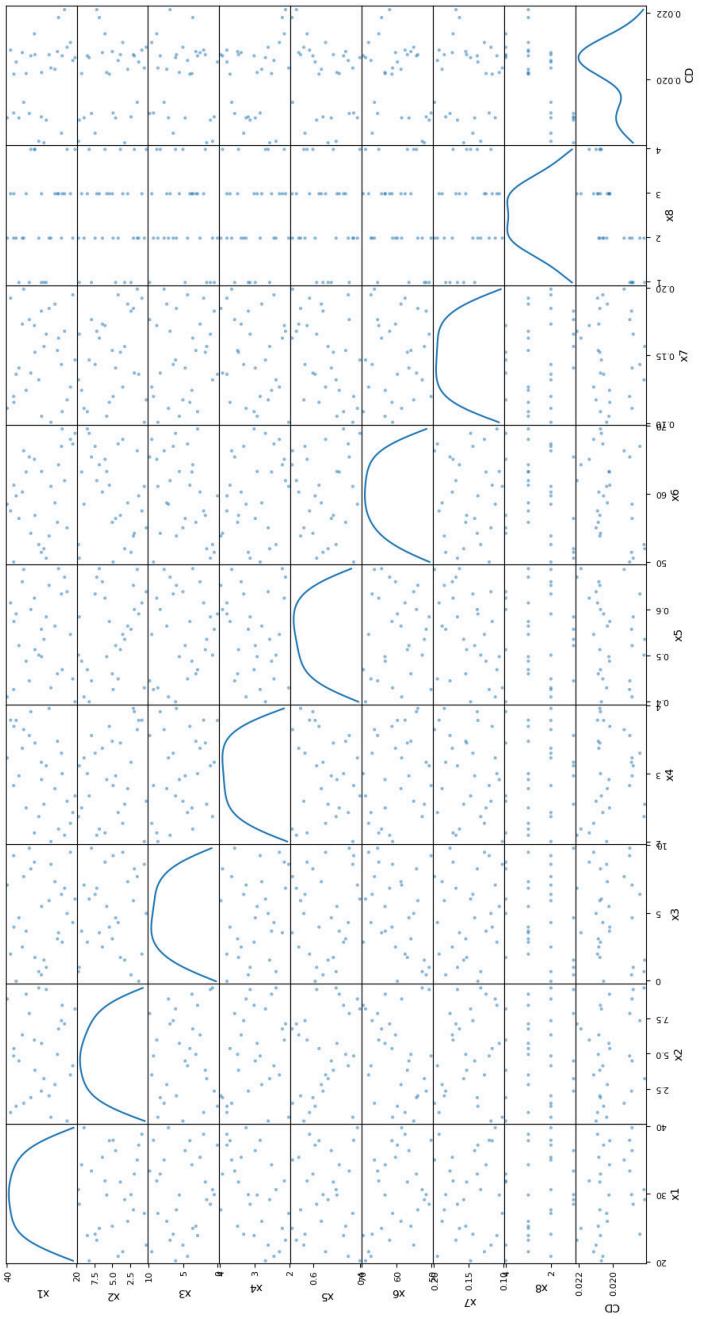

Fig. 11 Scatter Plot Matrix for CD.

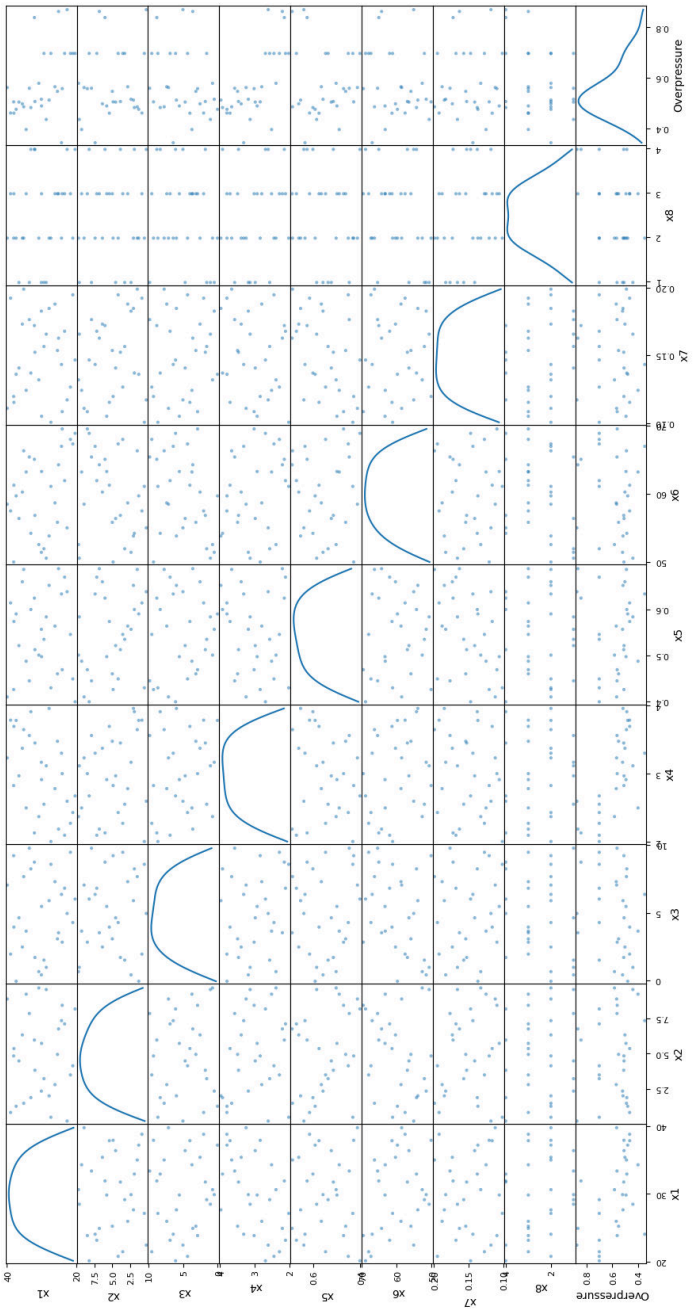

Fig. 12 Scatter Plot Matrix for Overpressure.

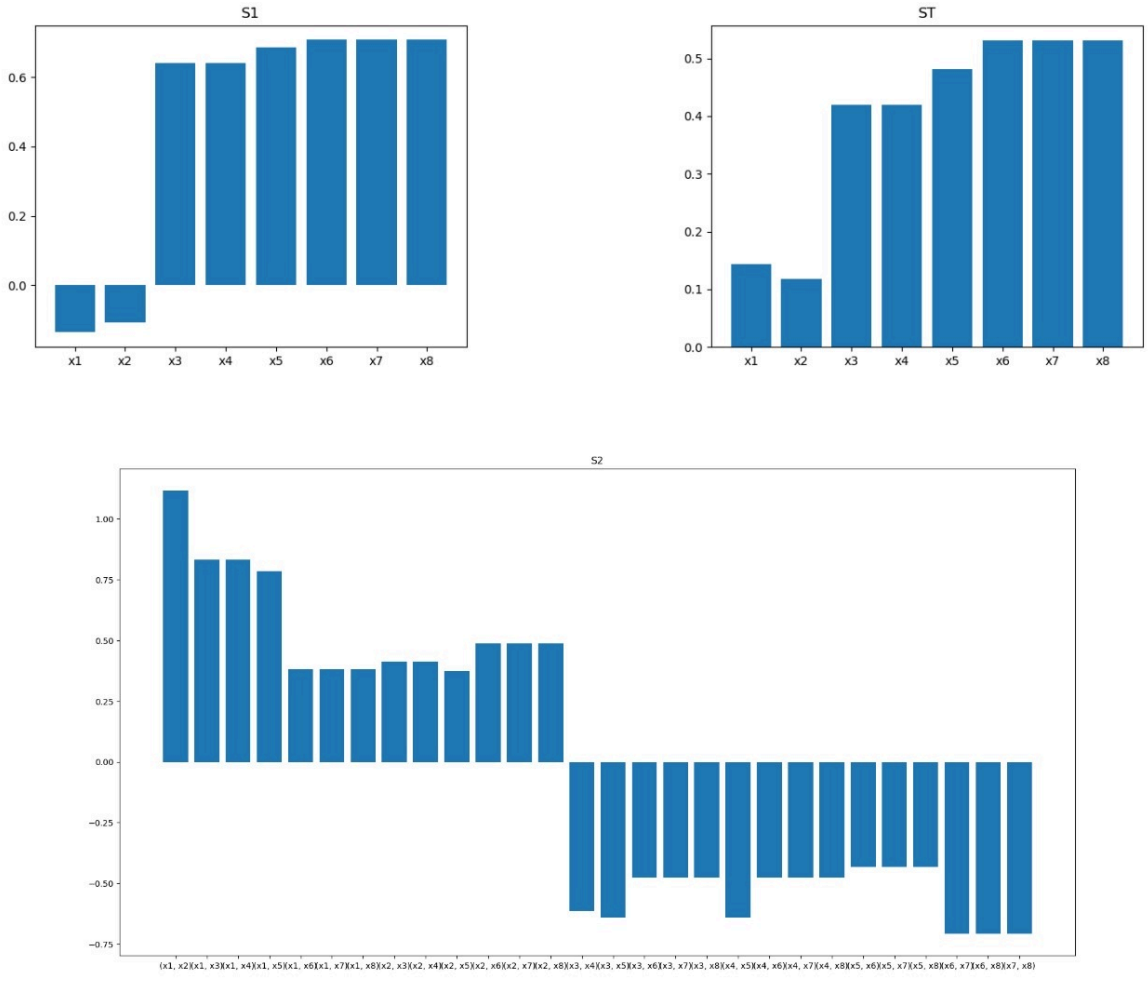

Fig. 13 CD Sobol's indices.

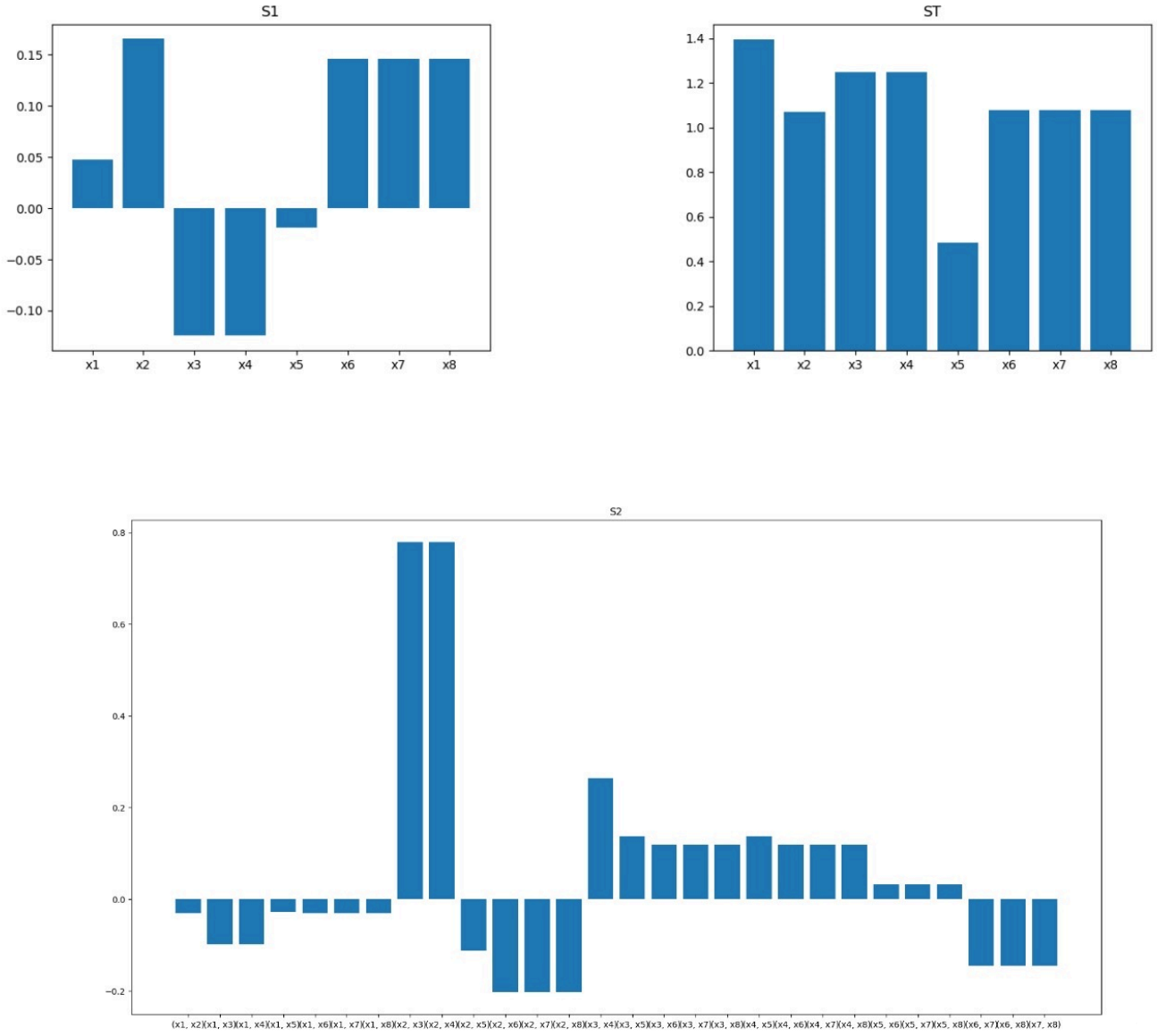

Fig. 14 Overpressure Sobol's indices.

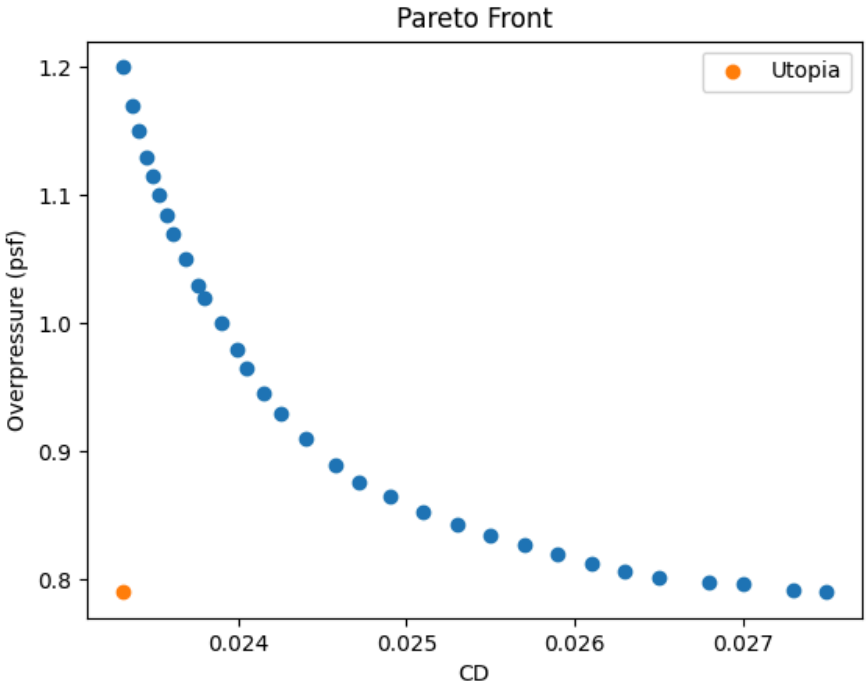

Fig. 15 Pareto front obtained by solving the Multi Objective Optimization problem.

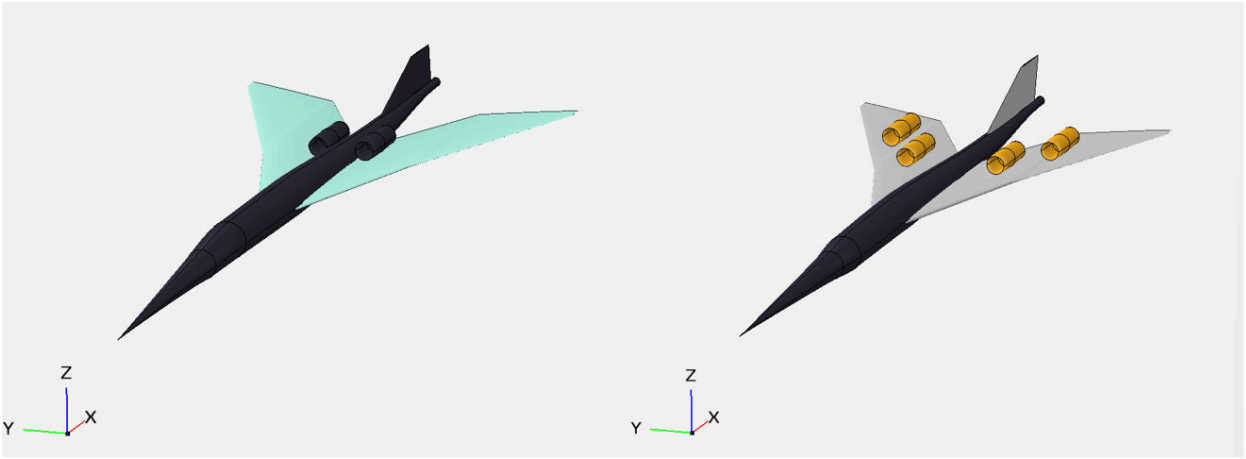

Fig. 16 D-1 business jet baseline configuration (left) and optimal solution (right).

Toward quieter and more efficient supersonic flight: multi-objective optimization of a Bell-Shaped Lift Distribution wing SSBJ

Bonavolontà, Giordana

2024-01-04

Bonavolontà G, Manoj A, Villena Munoz C, et al., (2024) Toward quieter and more efficient supersonic flight: multi-objective optimization of a Bell-Shaped Lift Distribution wing SSBJ. In: AIAA SCITECH 2024 Forum, 8-12 January 2024, Orlando, USA. Paper number AIAA 2024-2114
https://doi.org/10.2514/6.2024-2114